Directional Dependence of H/V Spectral Ratio of Microtremors Caused by Lateral Heterogeneity

S. Matsushima & H. Kawase
DPRI, Kyoto University, Japan

T. Hirokawa
Yamashita Sekkei, Inc., Japan

F.J. Sánchez-Sesma
Instituto de Ingeniería, Universidad Nacional Autónoma de México, Mexico

SUMMARY:
As observational evidence of 3-D Horizontal-to-Vertical (H/V) spectral ratio of microtremors, we show significant directional dependency at a site in Uji campus, Kyoto University, Japan, where the bedrock depth varies from east to west from 250m to 420m within 1 km. The observed NS/UD spectral ratio of microtremors is quite stable and has only one peak at around 0.5 Hz. On the other hand, the EW/UD spectral ratio of microtremors is smaller in amplitude and has higher peak frequency and sometimes two peaks. This directional dependence can be considered to be the result of 2-D surface geology. In order to investigate if the directional dependence in the Green's function in synthetics matches the observations, we performed various analyses using 1-D and 3-D point sources. We used a new theory proposed by the authors to calculate the H/V spectral ratio of microtremors assuming that the wave field is completely diffuse.

Keywords: H/V Spectral Ratio, Diffuse Field, Directional Dependence, Microtremor, Lateral Heterogeneity

1. INTRODUCTION

Horizontal-to-Vertical (H/V) spectral ratios of microtremors are useful to estimate the dominant frequency of a site and therefore are useful for site characterization and microzonation. They have been traditionally interpreted as representing either the Rayleigh wave ellipticity (Lermo and Chávez-García, 1994; Malischewsky and Scherbaum, 2004) or the S wave amplification directly (see e.g. Nakamura, 2000; Bonnefoy-Claudet, *et al*. 2008; Herat, 2008) for a horizontal stack of layers. However, based on the diffuse field theory (Perton *et al*., 2009), the H/V spectral ratio of microtremors corresponds to the square root of the ratio of the imaginary part of horizontal displacement for a horizontally applied unit harmonic load, $\mathrm{Im}[G_{11}]$, and the imaginary part of vertical displacement for a vertically applied unit harmonic load, $\mathrm{Im}[G_{33}]$ (Sánchez-Sesma *et al*., 2011).

In this paper, we explore the applicability of the diffuse field concepts to analyze microtremor records when there is lateral heterogeneity. We observed directional dependency of H/V spectral ratios that can be considered to be the result of non 1-D subsurface geology. For a sufficiently flat, horizontally layered structure, we can easily calculate the theoretical Green's function for that 1D model. Therefore, we can invert the underground structure below that site by using theoretical point source solution. On the other hand, for a laterally heterogeneous underground structure, the horizontal reflection responses are different (Uebayashi, 2003) and in order to interpret H/V spectral ratios for sites with lateral heterogeneity, a numerical approach such as 3-D finite-difference method (FDM) is needed. We performed several analyses by using the proposed idea of this study.

After preliminary 1-D analysis using a model with a horizontal stack of layers, we will perform 3-D point source analysis to see directional dependence in the Green's function similar to the observation using FDM.

2. MICROTREMOR OBSERVATION

We performed continuous microtremor measurements to obtain data in order to understand the velocity structure of Uji campus of Kyoto University, Kyoto, Japan, through analysis of H/V spectral ratios.

2.1. Conditions of Measurements and Analysis

We selected four sites to observe microtremors within the Uji campus (see Fig. 2.1). We used portable accelerometer SMAR-6A3P with external battery as shown in Photo 2.1 to observe microtremors. SMAR-6A3P consists of three accelerometers for two horizontal and one vertical component combined with a LS-8000WD data logger. We made observations with the following conditions; 100 Hz sampling, 500 times amplified, time correction with GPS, and consecutive time duration of 15 or 30 minutes with interval of the same duration. From the observed microtremor time series, we took out 40.96 second time window sections overlapping half of the time window, resulting of 42 time sections from 15 minutes and 84 time sections from 30 minutes of observation for the analysis. Then we calculated averaged H/V spectral ratios for each time section for NS and EW components separately and not by averaging the two horizontal components as done in conventional H/V spectral ratio studies. Finally, we averaged the H/V spectral ratio for each day of measurement.

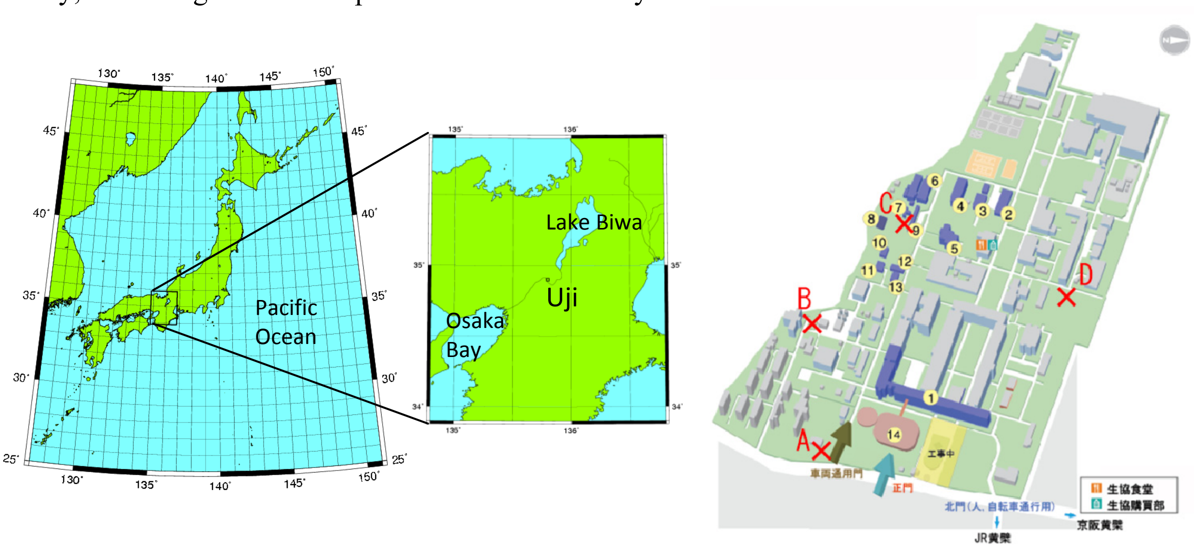

(a) Location of Uji (b) Map of Uji campus

Figure 2.1. Maps showing (a) the location of Uji, Kyoto, Japan and (b) the Uji campus of Kyoto University ("X" shows the microtremor measurement sites)

Photo 2.1. Example of microtremor measurement site using portable accelerometer SMAR-6A3P and external battery

2.2. Observed H/V Spectral Ratios

Fig. 2.2 shows the average H/V spectral ratio for NS/UD and EW/UD components separately for data of June 21st, 2010, at sites A to D shown in Fig. 2.1b. From the figures, we can see that for every site the peak ratio of NS/UD component at about 4.0 is larger than that of EW/UD component at about 2.5 and the peak frequency of NS/UD component at 0.5Hz is smaller than that of EW/UD component at 0.6Hz. For data of June 23rd, 2010, shown in Fig. 2.3, the peak frequency for NS/UD component is same at 0.5Hz as Fig. 2.2, but for EW/UD component, a second peak at about 0.4Hz appears along with the 0.6Hz peak. The NS/UD component looks more stable compared to EW/UD component.

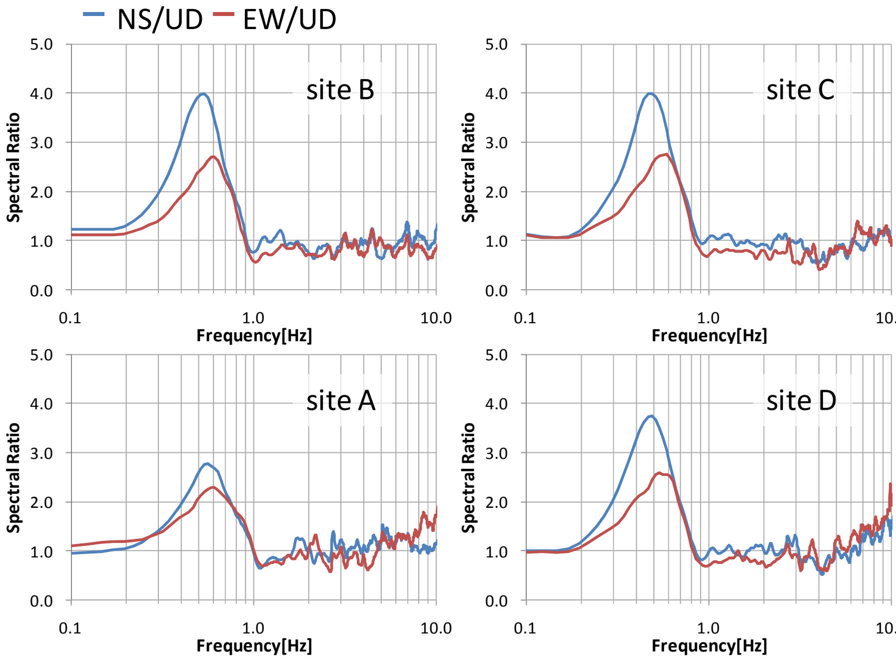

Figure 2.2. Average H/V spectral ratio of June 21st, 2010, observed at sites A to D in Fig. 2.1b

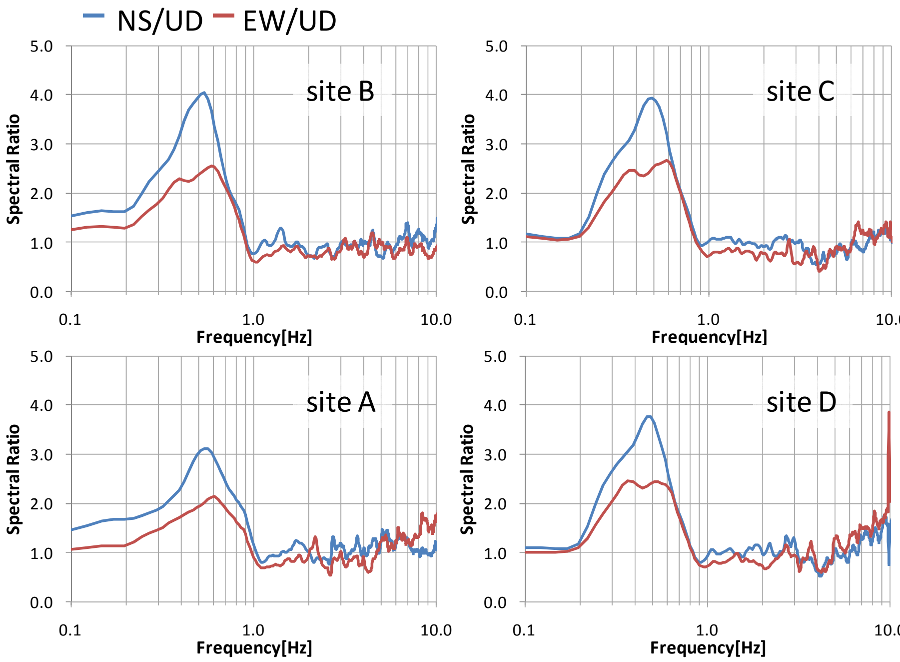

Figure 2.3. Average H/V spectral ratio of June 23rd, 2010, observed at sites A to D in Fig. 2.1b

Previous survey and research by Koizumi *et al*. (2002) show that the bedrock is dipping east to west from the Obaku fault running north-to-south just east of the campus. The bedrock depth beneath Uji campus varies from 250m to 420m within 1km distance as shown in Fig. 2.4. In the figure, the peak frequency of H/V spectral ratios are listed for NS/UD and EW/UD components in red and blue, respectively. The alphabets correspond to the names of the measurement sites in Fig. 2.1b. The peak frequency for the NS/UD component gets higher as the bedrock depth gets shallower, but for the EW/UD component it does not seem to depend on the depth of the bedrock. From this result, we may assume that the 2-D basin structure is playing a role in the difference between the NS/UD and EW/UD components. In order to verify our assumption, we checked the correspondence of the direction of the Obaku fault to the angle that the difference between two horizontal components becomes largest. By rotating the horizontal coordinate from 0 to 90 degrees we searched for the rotation angle that the ratio of amplitude of spectral ratio of NS/UD and EW/UD becomes smallest (see Fig. 2.5a). As a result, the lowest ratio between NS/UD and EW/UD was around 5 to 15 degrees. In Fig. 2.5b, we can see that the fault trace of Obaku fault is about N13.2E, so that the two angles are in good agreement.

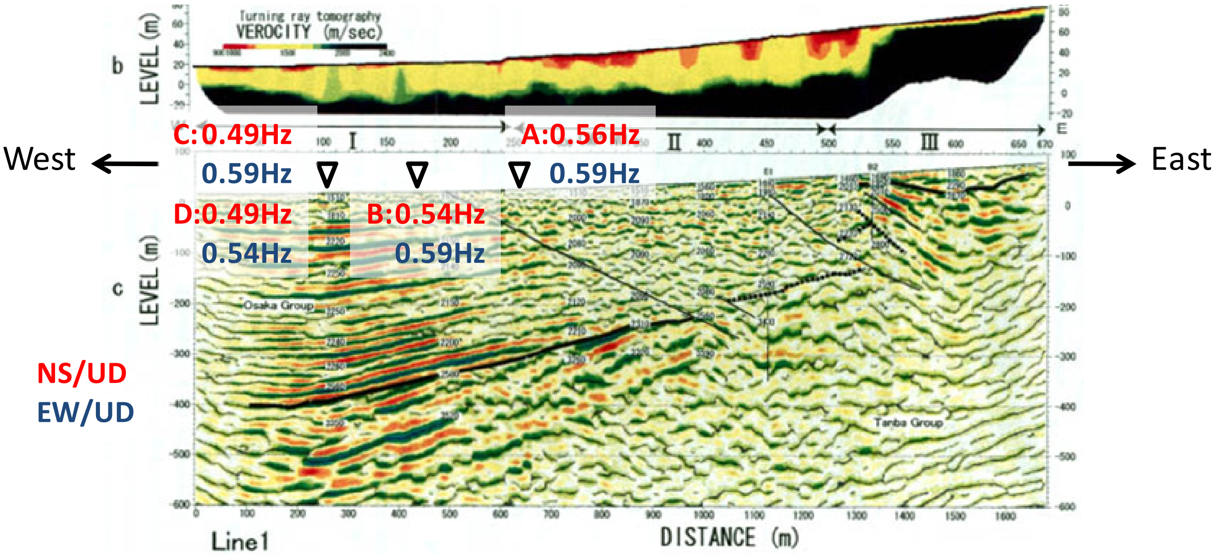

Figure 2.4. Section profile beneath Uji campus along the east-west survey line in Fig. 2.5b (After Koizumi *et al.*, 2002) and peak frequencies of average H/V spectral ratios of June 21st, 2010, observed at sites A to D in Fig. 2.1b

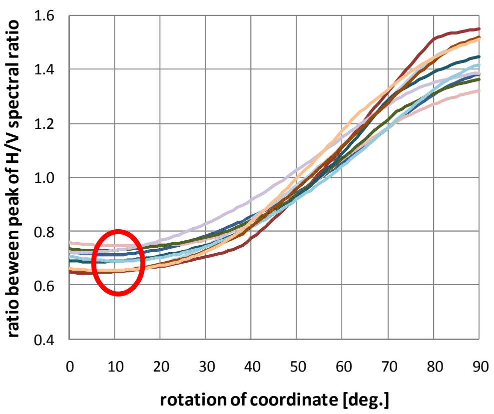

(a) Transition of difference of peak H/V spectral ratios according to rotation of coordinate

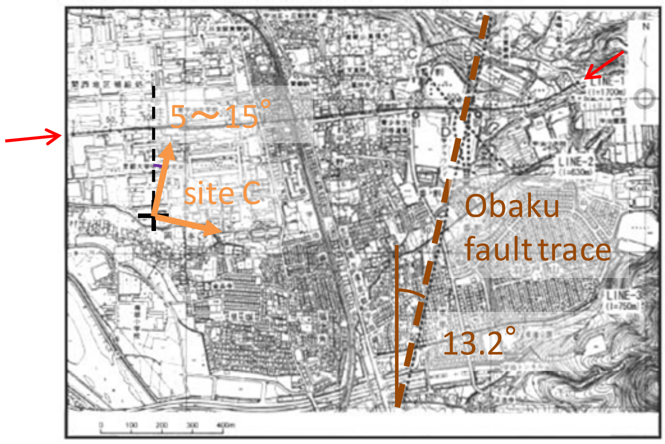

(b) Correspondence of rotation angle (after Koizumi *et al*., 2002)

Figure 2.5. Correspondence of rotation angle for lowest difference of peak H/V spectral ratio to the Obaku fault just east of Uji campus

3. THEORETICAL H/V SPECTRAL RATIO

In this section, we demonstrate our new proposed theory, that based on the diffuse field theory (Perton *et al.*, 2009) the microtremor H/V spectral ratio corresponds to the square root of the ratio of the imaginary part of horizontal displacement for a horizontally applied unit harmonic load, $\mathrm{Im}[G_{11}]$, and the imaginary part of vertical displacement for a vertically applied unit load, $\mathrm{Im}[G_{33}]$ (Sánchez-Sesma *et al.*, 2011). We will also show the comparison between theoretical and observed H/V spectral ratio.

3.1. Formulation of Theoretical H/V Spectral Ratio Based on Diffuse Field Theory

Within a 3-D diffuse, equipartitioned field, the average cross correlations of displacement at points $\mathbf{x}_\mathrm{A}$ and $\mathbf{x}_\mathrm{B}$ can be written as;

$$\langle u_i(\mathbf{x}_\mathrm{A},\omega)u^*{}_j(\mathbf{x}_\mathrm{B},\omega)\rangle = -2\pi E_S k^{-3}\mathrm{Im}\left[G_{ij}(\mathbf{x}_\mathrm{A},\mathbf{x}_\mathrm{B},\omega)\right] \tag{3.1}$$

where $\mathbf{x}_\mathrm{A}$ and $\mathbf{x}_\mathrm{B}$ are position vectors, ω is circular frequency, u_i is displacement in direction i, * means complex conjugate, angular brackets ($\langle\ \ \rangle$) denote azimuthal average, $E_S = \rho\omega^2 S^2$ is energy density of S waves, $k = \omega/\beta$ is wavenumber of S waves, β is S wave velocity, S^2 is average spectral density of S waves. Green's function $G_{ij}(\mathbf{x}_\mathrm{A},\mathbf{x}_\mathrm{B},\omega)$ is displacement at $\mathbf{x}_\mathrm{A}$ in direction i produced by a unit load at $\mathbf{x}_\mathrm{B}$ in direction j (Sánchez-Sesma *et al.*, 2011a). In order to calculate the theoretical energy density at a given point $\mathbf{x}_\mathrm{A}$, we rewrite Eqn. 3.1 assuming $\mathbf{x}_\mathrm{A} = \mathbf{x}_\mathrm{B}$ as;

$$E(\mathbf{x}_\mathrm{A}) = \rho\omega^2\langle u_m(\mathbf{x}_\mathrm{A})u^*{}_m(\mathbf{x}_\mathrm{A})\rangle = -2\pi\mu E_S k^{-1}\mathrm{Im}[G_{mm}(\mathbf{x}_\mathrm{A},\mathbf{x}_\mathrm{A})] \tag{3.2}$$

where μ is shear modulus. Eqn. 3.2 is valid even if the summation convention is ignored (Perton *et al.*, 2009), so $E(\mathbf{x}_\mathrm{A})$ can be written as $E_m(\mathbf{x}_\mathrm{A})$, which is directional energy density (DED) along direction m.

We may express the H/V spectral ratio in terms of energy densities. For instance, $E_1(\mathbf{x},\omega)$ is proportional to $\langle u_1{}^2\rangle = \langle H_1{}^2\rangle$. It is common to eliminate the angular brackets while writing the expression for the average H/V spectral ratio as;

$$\frac{H(\omega)}{V(\omega)} = \sqrt{\frac{E_1(\mathbf{x},\omega) + E_2(\mathbf{x},\omega)}{E_3(\mathbf{x},\omega)}} \tag{3.3}$$

where E_1, E_2 and E_3 are the energy densities and the subscripts 1 and 2 refer to horizontal and 3 to vertical degrees of freedom. Eqn 3.3 is the form adopted by Arai and Tokimatsu (2004).

If we assume that microtremors constitute a diffuse field, the average spectral densities may be regarded as DEDs and then we may invoke the connection between the normalized averages of energy densities of diffuse field with the imaginary part of Green's function at the source (Sánchez-Sesma *et al.*, 2011). In fact, from Eqns. 3.2 and 3.3 we can write;

$$\frac{H(\omega)}{V(\omega)} = \sqrt{\frac{\mathrm{Im}[G_{11}(\mathbf{x},\mathbf{x};\omega)] + \mathrm{Im}[G_{22}(\mathbf{x},\mathbf{x};\omega)]}{\mathrm{Im}[G_{33}(\mathbf{x},\mathbf{x};\omega)]}} \tag{3.4}$$

This equation (Sánchez-Sesma *et al.*, 2011) shows average microtremor H/V spectral ratio corresponds to the square root of the ratio of the imaginary part of horizontal displacement for a horizontally applied unit harmonic load, $\mathrm{Im}[G_{11}]$ and $\mathrm{Im}[G_{22}]$, and the imaginary part of vertical displacement for a vertically applied unit load, $\mathrm{Im}[G_{33}]$.

3.2. 1-D Analysis Considering the Velocity Model of Uji Campus

In order to check the validity of the theory, we calculated theoretical H/V spectral ratio based on our theory assuming a 1-D structure at one of the microtremor measurement sites in Uji campus, site C. Fig. 3.1 shows the velocity profile obtained from VSP survey near site C in light lines (Iwata *et al.*, 2001). We assumed a simple 3 layered 1-D velocity model as shown in Table 3.1 denoted by dark lines in Fig. 3.1 according to the results of the VSP survey. Red and blue lines are the P wave and S wave velocity, respectively. The theoretical H/V spectral ratio calculated from the velocity model is shown in Fig. 3.2 with black line. In the figure, we also plot the H/V spectral ratio based on ellipticity of Rayleigh waves (gray line) from the same velocity model as well as the observed microtremor H/V spectral ratio (red and blue lines for NS/UD and EW/UD components, respectively). We can see that the theoretical H/V spectral ratio fit that of the observed NS/UD component which can be interpreted as 1-D structure. Also, the peak and the dip frequency of the H/V spectral ratio derived from the ellipticity of Rayleigh waves match both the theory and observation.

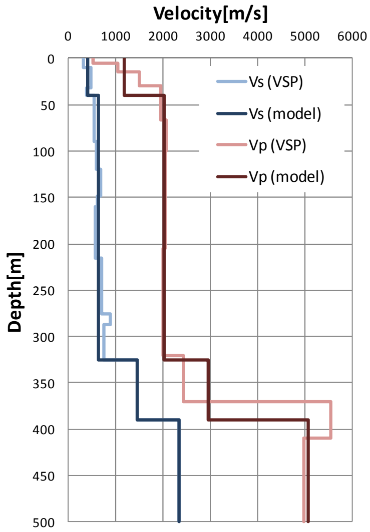

Figure 3.1. Velocity profile from VSP survey near site C (light lines) and assumed 1-D velocity model with 3 layers (dark lines)

Table 3.1. Three-layered 1D velocity model at site C

Layer	thickness [m]	Vp [m/s]	Vs [m/s]	density [kg/m^3]	Q
1	40	1,177	406	1,900	100
2	285	2,209	638	1,900	100
3	65	2,950	1,450	2,100	100
Bedrock	-	5,083	2,348	2,600	100

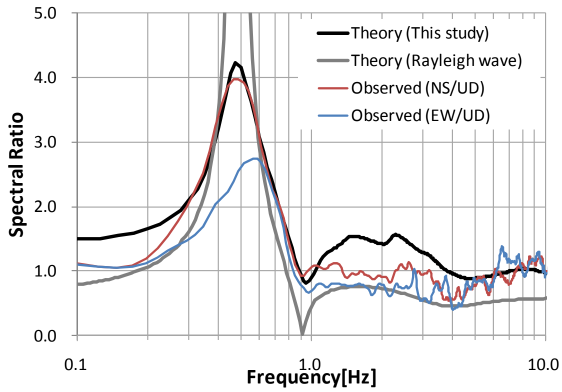

Figure 3.2. Theoretical H/V spectral ratio (black line) compared against H/V spectral ratio derived from ellipticity of Rayleigh waves (gray line) and observed H/V spectral ratio of June 21st, 2010 (red and blue lines)

4. NUMERICAL 3D H/V SPECTRAL RATIO

In order to take in account of the 2-D or 3-D subsurface structure, we need to incorporate a numerical approach. In this study we use 3-D staggered-grid FDM (Graves, 1996; Graves and Day, 2003) to study cases of laterally heterogeneous elastic layers over a half-space.

4.1. Layered 1-D Velocity Model

For calibration purposes, we first checked that numerical calculations by FDM give the same results as theoretical ones. We assume a flat-layered model with a single layer over half-space, equivalent to site C. The condition for 3-D FDM calculation is listed in Table 4.1 and the velocity model for the flat-layered case is listed in Table 4.2. Fig. 4.1a displays the schematic image of the velocity model of the one layer 1-D model. We apply a unit load to the surface of the model at the target position and retrieve the imaginary part of the Green's function from the response at the same position.

Figure 4.2 shows the comparison of theoretical and numerical results for 1-D velocity model shown in Table 4.2 and Fig. 4.1a. Figure 4.2a is the imaginary part of Green's function for horizontal (dark line) and vertical (light line) components. The blue and orange lines are for FDM and theoretical results, respectively. The FDM results shows fairly good match to the theoretical one. Figure 4.2b is the H/V spectral ratio derived from the imaginary part of Green's function shown in Fig. 4.2a. Since the imaginary part of Green's function match each other, the H/V spectral ratio also shows good match, naturally.

Table 4.1. Conditions of 3-D FDM calculation

parameter	order of spatial accuracy	model size [km]	grid spacing [m]	total grids	low pass filter	time increment [sec]	time steps	total duration [sec]	absorbing boundary
value	4	length 4 width 4 depth 4	10	32 million	13.0 Hz	0.007	30000	21.0	25 grids

Table 4.2. One layer 1-D velocity model equivalent of site C for testing FDM calculation

Layer	Thickness [m]	Vp [m/s]	Vs [m/s]	Density [kg/m^3]	Q
1	390	1,985	661	1,930	9999
Bedrock	-	5,083	2,348	2,600	9999

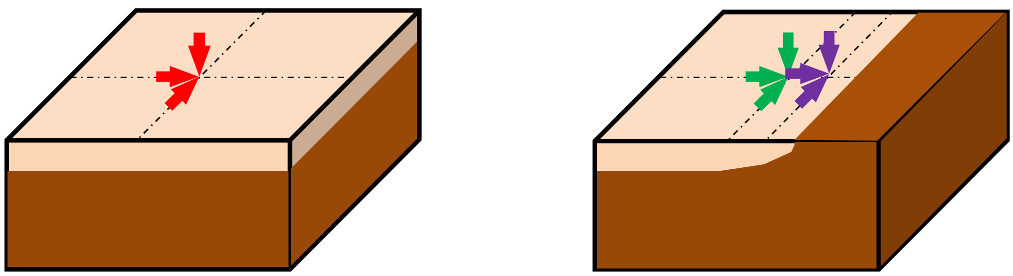

(a) One layer 1-D velocity model (b) One layer 2-D velocity model

Figure 4.1. Schematic image of (a) One layer 1-D velocity model and (b) One layer 2-D model, used for 3-D FDM calculation

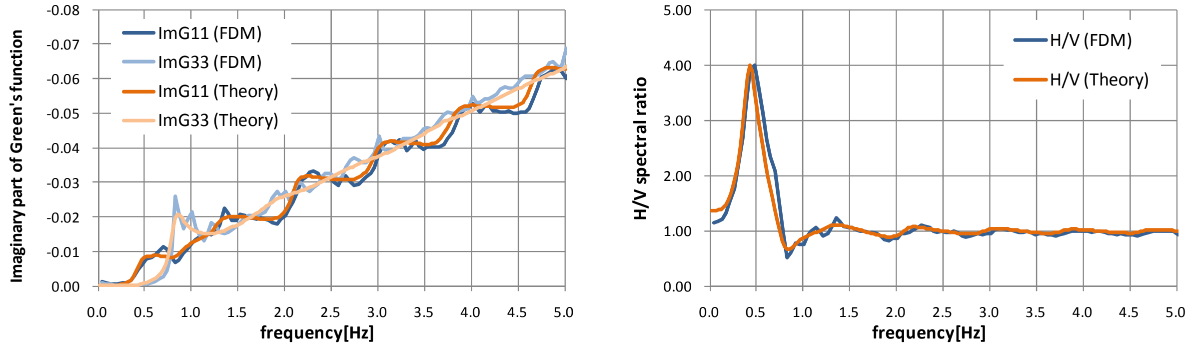

(a) Imaginary part of Green's function (b) H/V spectral ratio

Figure 4.2. Comparison of (a) imaginary part of Green's function and (b) H/V spectral ratio of theoretical and numerical results for 1-D velocity model in Table 4.2

4.2. Layered 2-D Velocity Model

Now we consider a laterally heterogeneous velocity structure. We use a 2-D velocity model and calculate the 3-D wave field. The 2-D velocity model consists of one layer over half-space that gradually gets shallow from west to east and eventually pinches out at 1,200m (120grids) from the boundary of the model as shown in Fig. 4.1b. The maximum depth of the 2-D basin model is 420m. The parameters of the model are listed in Table 4.3. For this model, we first calculated the H/V spectral ratio at position of site C, which corresponds to the green arrow in Fig. 4.1b. The H/V spectral ratio for this case is shown in Fig. 4.3a. The H/V spectral ratio for NS/UD and EW/UD components do not have large difference as expected from the observed H/V spectral ratio at site C.

Next, we did the same calculation except we moved the target position 620m (62 grids) to the east, closer to the basin edge as shown by the purple arrows in Fig 4.1b. The H/V spectral ratio for this case is shown in Fig. 4.3b. We can see that for this case the NS/UD and EW/UD components have large difference corresponding to the difference seen in the observed H/V spectral ratio.

Table 4.3. One layer 2-D velocity model

Layer	Thickness [m]	Vp [m/s]	Vs [m/s]	Density [kg/m^3]	Q
1	< 420	1,985	661	1,930	9999
Bedrock	-	5,083	2,348	2,600	9999

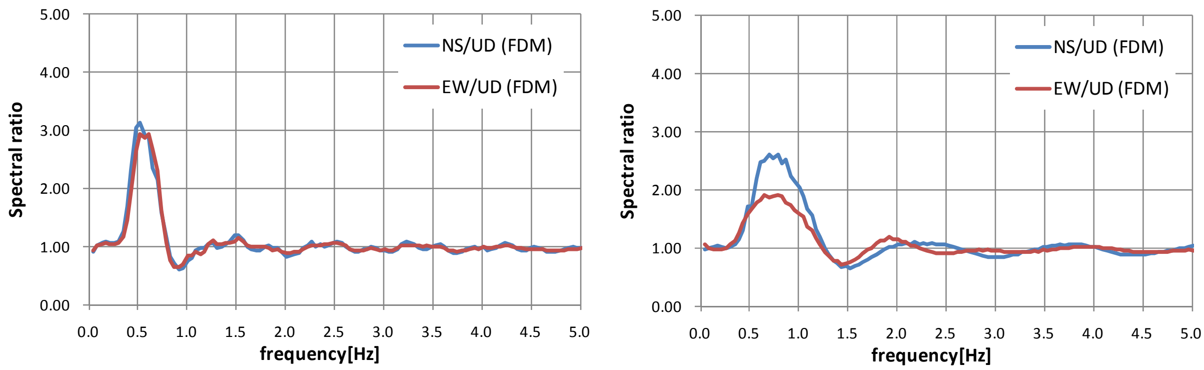

(a) site C (b) site 620m east of site C (closer to the edge)

Figure 4.3. Comparison of H/V spectral ratio of NS/UD and EW/UD at (a) site C and (b) site 620m east of site C closer to the edge, calculated by FDM for 2-D basin model

5. DISSCUSSION AND CONCLUSIONS

From the H/V spectral ratios of microtremor data obtained at Uji campus of Kyoto University, Kyoto, Japan, we confirmed directional dependency that seems to correspond to the deep 2-D basin structure. The NS/UD component which is parallel to the strike of Obaku fault, has larger peak and lower peak frequency compared to the EW/UD component, which is perpendicular to the fault trace and the 2-D basin structure. Assuming a 1-D structure beneath Uji campus, the theoretical H/V spectral ratio fit the NS/UD component of the data. This shows that the NS/UD component acts as same as a 1-D site but on the other hand, the EW/UD component is affected by the 2-D basin structure and acts differently. In order to simulate the H/V spectral ratio for site with lateral heterogeneity, we used 3-D FDM to numerically calculate Green's function to derive numerical H/V spectral ratio by the same procedure as theoretical H/V spectral ratio. From the comparison with theoretical and observational H/V spectral ratios, we confirmed the validity to use FDM to calculate numerical H/V spectral ratio from imaginary part of Green's function for sites with lateral heterogeneity.

Although we succeeded in simulating the difference between the orthogonal two horizontal components of the microtremor H/V spectral ratio qualitatively, the H/V spectral ratios obtained using the assumed 2-D basin model from FDM calculation cannot explain the observed data. This may be the indication that the actual bedrock may have steeper dip than the model used in this study, or has a shallow layer with large contrast not included in the model.

ACKNOWLEDGEMENTS

The authors thank deeply Professor Tomotaka Iwata of Kyoto University for permission to use VSP data and to Dr. Robert W. Graves of USGS for the use of his FDM code. Partial support from DGAPA-UNAM under projects IN121709 and IN104712 is gratefully acknowledged.

REFERENCES

Arai, H. and Tokimatsu, K. (2004). S-Wave Velocity Profiling by Inversion of Microtremor H/V Spectrum, *Bull. Seism. Soc. Am.*, **Vol. 94:1**, 53–63.

Bonnefoy-Claudet, S., Köhler, A., Cornou, C., Wathelet, M. and Bard, P.-Y. (2008). Effects of Love Waves on Microtremor H/V Ratio, *Bull. Seism. Soc. Am.*, **Vol. 98:1**, 288-300.

Graves, R.W. (1996). Simulating seismic wave propagation in 3D elastic media using staggered-grid finite differences, *Bull. Seism. Soc. Am.*, **Vol. 86:4**, 1091-1106.

Graves, R.W. and Day, S.M. (2003). Stability and Accuracy Analysis of Coarse-Grain Viscoelastic Simulations, *Bull. Seism. Soc. Am.*, **Vol. 93:1**, 283-300.

Herat, M. (2008). Model HVSR - A Matlab® Tool to Model Horizontal-to-Vertical Spectral Ratio of Ambient Noise, *Computers & Geosciences*, **Vol. 34**, 1514-1526.

Iwata, T., Honda, R., Irikura, K., Sato, T., Sawada, S., Nakashima, M., Yamada, K. and Aizawa, T. (2001). Small-Aperture 3D Seismic Array Observation in SE Kyoto Basin, *Proc. Seism. Soc. Japan 2001 Fall Meeting*, P094.

Koizumi, N., Tsukuda, E., Takahashi, M., Yokota, H., Iwata, T., Irikura, K., Uesuna, S., Takagi, K. and Hasegawa, M. (2002). Structural Profile of the Oubaku Fault, *Zisin 2*, **Vol. 55:2**, 153-166 (in Japanese with English abstract).

Lermo, J. and Chávez-García, F. J. (1994). Are Microtremors Useful in Site Response Evaluation?, *Bull. Seism. Soc. Am.*, **Vol. 84:5**, 1350-1364.

Malischewsky, P.G. and Scherbaum, F. (2004). Love's Formula and H/V-Ratio (Ellipticity) of Rayleigh Waves, *Wave Motion*, **Vol. 40: 1**, 57-67.

Nakamura, Y (2000). Clear identification of fundamental idea of Nakamura's technique and its applications, *Proc. 12th World Conf. on Earthq. Eng.*, New Zeland (CD-ROM), paper no. 2656.

Perton, M., Sánchez-Sesma, F. J., Rodríguez-Castellanos, A., Campillo, M. and Weaver, R. L. (2009). Two Perspectives on Equipartition in Diffuse Elastic Fields in Three Dimensions, *J. Acoust. Soc. Am.*, **Vol. 126:3**, 1125-1130.

Sánchez-Sesma, F. J., Rodríguez, M., Iturrarán-Viveros, U., Luzón, F., Campillo, M., Margerin, L., García-Jerez, A., Suarez, M., Santoyo, M. A. and Rodríguez- Castellanos, A. (2011). A theory for microtremor H/V spectral ratio: Application for a layered medium, *Geophys. J. Int. Exp. Lett.*, **Vol. 186:1**, 221-225, doi: 10.1111/j.1365-246X.2011.05064.x.

Uebayashi, H. (2003). Extrapolation of Irregular Subsurface Structures Using the Horizontal-to-Vertical Spectral Ratio of Long-Period Microtremors, *Bull. Seism. Soc. Am.*, **Vol. 93:2**, 570–582.